Journal of Applied Sciences

ISSN 1812-5654

Journal of Applied Sciences 9 (16): 2877-2886, 2009
ISSN 1812-5654

Air Fuel Ratio on Engine Performance and Instantaneous Behavior of Crank Angle for Four Cylinder Direct Injection Hydrogen Fueled Engine

M.M. Rahman, M.K. Mohammed and R.A. Bakar
Automotive Excellence Center, Faculty of Mechanical Engineering, Universiti Malaysia Pahang, Tun Abdul Razak Highway, 26300 Gambang, Kuantan, Pahang, Malaysia

Abstract: The present study focuses on the effect of air-fuel ratio and instantaneous behavior on crank angle of four cylinder direct injection hydrogen fueled engine. GT-Power was utilized to develop the model for direct injection engine. Air-fuel ratio was varied from rich limit (AFR = 27.464) to a lean limit (AFR = 171.65). The rotational speed of the engine was varied from 2500 to 4500 rpm. It can be seen from the obtained results that the air fuel ratio are greatly influence on the Brake Mean Effective Pressure (BMEP), Brake Efficiency (BE), Brake Specific Fuel Consumption (BSFC) as well as the maximum cylinder temperature. It can be seen that the decreases of BMEP, BE and maximum cylinder temperature with increases of air fuel ratio and speed, however increases the brake specific fuel consumption. For rich mixtures (low AFR), BMEP decreases almost linearly, then BMEP falls with a non-linear behavior. It can be observed that the brake thermal efficiency is increases nearby the richest condition (AFR ≅ 35) and then decreases with increases of air fuel ratio. Maximum of 35.4% at speed 2500 rpm can be seen compared with 26.3% at speed 4500 rpm. The optimum minimum value of BSFC occurred within a range of AFR from 38.144 (θ = 0.9) to 49.0428 (θ = 0.7) for the selected range of speed. The effect of the rotational speed on the instantaneous behavior of the cylinder pressure is no significant. The flame development, propagation and termination period consumes about 5 and 90% of the air fuel mixture and finally flame termination period which consumes about the rest of the mixture (5%). The present contribution suggests the direct injection fuel supply system as a strong candidate for solving the power and abnormal combustion problems.

Key words: Hydrogen fueled engine, direct injection, air fuel ratio, engine performance, crank angle, rotational speed

INTRODUCTION

With increasing concern about energy shortage and environmental protection, research on improving engine fuel economy and reducing exhaust emissions has become the major researching aspect in combustion and engine development. Due to limited reserves of crude oil, development of alternative fuel engines has attracted more and more concern in the engine community. Alternative fuels usually belong to clean fuels compared to diesel fuel and gasoline fuel in the combustion process of engines. The introduction of these alternative fuels is beneficial to slowing down the fuel shortage and reducing engine exhaust emissions. Hydrogen fuel is regarded as one of the most promising alternative fuels for automobiles in future. Technology of the optimum control on hydrogen-fueled engines is a key to improve its performances in every respect. An important issue with energy usage is the associated undesirable emissions. High flame speed leading to good thermal efficiency, wide flammability limits, absence of carbon based emissions, qualitative mixture control and high diffusivity leading to good mixing are some of advantages of hydrogen. Hydrogen induction techniques play a very dominant and sensitive role in determining the performance characteristics of the hydrogen fueled internal combustion engine (Suwanchotchoung, 2003). Hydrogen fuel delivery system can be broken down into three main types including the carbureted injection, Port Fuel Injection (PFI) and Direct Injection (DI) (COD, 2001). In direct injection, the intake valve is closed when the fuel is injected into the combustion cylinder during the compression stroke (COD, 2001). Like PFI, direct injection has long been viewed as one of the most attractive choices for supplying hydrogen fuel to combustion chamber (White *et al.*, 2006; Verhelst *et al.*, 2006;

Corresponding Author: M. M. Rahman, Faculty of Mechanical Engineering, Universiti Malaysia Pahang, Tun Abdul Razak Highway, 26300 Gambang, Kuantan, Pahang, Malaysia
Tel: +6-09-5492207 Fax: +6-09-5492244

Zhenzhong *et al*., 2002; Mohammadi *et al*., 2007; Guo *et al*., 1999; Jorach *et al*., 1997; Kim *et al*., 1995). This view is based on: its prevention for abnormal combustion: pre-ignition, backfire and knock; and the high volumetric efficiency, (since hydrogen is injected after intake valve closing). The improved volumetric efficiency and the higher heat of combustion of hydrogen compared to gasoline, provides the potential for power density to be approximately 115% that of the identical engine operated on gasoline (White *et al*., 2006). However, it is worthy to emphasize that while direct injection solves the problem of pre-ignition in the intake manifold, it does not necessarily prevent pre-ignition within the combustion chamber (COD, 2001). In fact the difficulties and limitations accompanied with DI are more serious and severe than those of PFI. Direct injection during the compression stroke needs high pressure hydrogen and thus effectively requires liquid hydrogen storage. Metal hydrides can only provide low pressure hydrogen, compressed hydrogen could be used but this limits the effective tank contents as the tank can only be emptied down to the fuel injection pressure. Compressing gaseous hydrogen on board would mean an extra compressor and a substantial energy demand (Verhelst, 2005). Furthermore, a high-pressure, high flow-rate hydrogen injector is required for operation at high engine speeds and to overcome the in-cylinder pressure for injection late in the compression stroke. The high pressure was defined by White *et al*. (2006) as greater than 80 bar to ensure sonic injection velocities and high enough mass flow rates for Start of Injection (SOI) throughout the compression stroke. The need for rapid mixing necessitates the use of critical flow injectors and the short time duration with late injection requires high mass flow rates. The valve leakage at the valve seat and the losses associated with the injection system are another issues (Kim *et al*., 1995; Tsujimura *et al*., 2003; Kim *et al*., 2006). Guo *et al*. (1999) have kept the injector in a status such that it is always not under a high pressure, so pre-ignition caused by the injector's leakage at initial stage of starting the engine was avoided. While, a seal made of an elastomer material has been used with success to prevent valve leakage at the valve seat (Homan *et al*., 1983; Green and Glasson, 1992). It is apparent that the structure of DI system is more sophisticated, expensive and attend great durability problem (COD, 2001; Stockhausen *et al*., 2002; Yi *et al*., 1996).

Another important challenge for DI is the extremely short time for hydrogen-air mixing. For early injection (i.e., coincident with Inlet Valve Closure (IVC) maximum available mixing times range from approximately 20-4 msec across the speed range 1000-5000 rpm, respectively (White *et al*., 2006). This insufficient time leads to unstable engine operation at low hydrogen-air equivalence ratios due to insufficient mixing between hydrogen and air (Rottengruber *et al*., 2004). As an attempt to fix this problem, Guo *et al*. (1999) used a fast response high pressure solenoid valve to improve hydrogen jet penetration and mixture formation in the combustion chamber and to prevent backfire occurring in the hydrogen supply pipe between the valve and the combustion chamber. Jorach *et al*. (1997) suggested early injection to provide more time for mixing process. However, in practice, to avoid preignition, SOI is retarded with respect to IVC and mixing times are further reduced (White *et al*., 2006).

Among the subsequent problems of the inadequate mixing time for DI system, is the unacceptable high level of NOx emissions. The low grade of homogenization is responsible for forming rich areas in the combustion chamber. The reaction temperatures in these rich areas may rise up more than 2300 K (Jorach *et al*., 1997). Several researchers have tried to surmount this problem via proper adjusting for injection time. Late injection, as a solution, was investigated by Mohammadi *et al*. (2007) and Jorach *et al*. (1997). However, this measure is insufficient and the system will be susceptible for pre-ignition as stated above. Therefore, additional transactions like utilization of other techniques such as EGR and after-treatment methods are required to bring the NOx emission to acceptable level (Mohammadi *et al*., 2007).

As a whole, both PFI and DI have their advantages and disadvantages. DI is better for full load performance (maximum power output), PFI is better at part load (maximum engine efficiency) (Verhelst, 2005; Verhelst *et al*., 2006). Some designs proposed utilizing dual-injection (both of PFI and DI) in the same engine (Kim *et al*., 2006; Yi *et al*., 2000; Blair, 1999). The dual-injection strategy was suggested to take advantage of the high thermal efficiencies at low and medium loads with PFI system and the high power output with DI system. (White *et al*., 2006). Kim *et al*. (2006) introduced the following strategy: using PFI only under idling and low load because no backfire occurs. For the case of high load, most of the fuel is injected directly into the cylinder during the compression process and the rest, which guarantees that the intake mixture is lean enough so, that no backfire occurs, is supplied into the intake pipe to increase the mixing rate. Excellent results were reported, such that the maximum torque of the dual-injection was increased by about 60% compared to a hydrogen engine using external mixture preparation and the brake thermal efficiency was higher by about 22% at low load compared with direct-cylinder injection hydrogen engine. The objectives of this study are to investigate the effect of air fuel ratio on engine performance and instantaneous behavior of intake, exhaust port pressure and cylinder pressure on the crank angle of the direct injection hydrogen fueled engine.

MATERIALS AND METHODS

This study was conducted at high computing laboratory, Automotive Excellence Centre, Faculty of Mechanical Engineering, Universiti Malaysia Pahang, Kuantan in 2008.

Hydrogen engine modeling

Engine performance parameters: The Brake Mean Effective Pressure (BMEP) can be defined as the ratio of the brake work per cycle W_b to the cylinder volume displaced per cycle V_d and it can be expressed as in Eq. 1 (Heywood, 1988):

$$BMEP = \frac{W_b}{V_d} \tag{1}$$

Equation 1 can be rewrite for the four stroke engine as in Eq. 2:

$$BMEP = \frac{2P_b}{NV_d} \tag{2}$$

where, P_b is the brake power and N is the rotational speed. Brake efficiency (η_b) can be defined as the ratio of the brake power P_b to the engine fuel energy as in Eq. 3:

$$\eta_b = \frac{P_b}{\dot{m}_f(LHV)} \tag{3}$$

where, $\dot{m}_f$ is the fuel mass flow rate and LHV is the lower heating value of hydrogen.

The Brake Specific Fuel Consumption (BSFC) represents the fuel flow rate $\dot{m}_f$ per unit brake power output and can be expressed as in Eq. 4 (Heywood, 1988):

$$BSFC = \frac{\dot{m}_f}{P_b} \tag{4}$$

The volumetric efficiency (η_v) of the engine defines as the mass of air supplied through the intake valve during the intake period ($\dot{m}_a$) by comparison with a reference mass, which is that mass required to perfectly fill the swept volume under the prevailing atmospheric conditions and can be expressed as in Eq. 5:

$$\eta_v = \frac{\dot{m}_a}{\rho_{ai} V_d} \tag{5}$$

where, ρ_{ai} is the inlet air density.

The burning rate (X_b) of combustion process was modeled using Wiebe function, which can be expressed as Eq. 6:

$$X_b = 1 - \exp[-a\left(\frac{\theta - \theta_i}{\Delta\theta}\right)^{n+1}] \tag{6}$$

where, θ is the crank angle, θ_i is the start of combustion, $\Delta\theta$ is the combustion period and a and n are adjustable constants.

Furthermore, the heat transfer in-side the cylinder was modeled using a formula which is closely emulates the classical Woschni correlation. Based on this correlation, the heat transfer coefficient h_c can be expressed as Eq. 7:

$$h_c = 3.26B^{-0.2}\, p^{0.8}\, T^{-0.55}\, w^{0.8} \tag{7}$$

where, B is the bore in meters, p is the pressure in kPa, T is temperature in K and w is the average cylinder gas velocity in m sec^{-1}.

The hydrogen gas fuel was injected directly in-side the cylinders using the four sequential pulse fuel injectors. The AFR was imposed for the injectors. Then, the injected fuel rate was estimated using the Eq. 8 (Ferguson and Kirkpatrick, 2001):

$$\dot{m}_{delivery} = \eta_v \ell_{ref}\, NV_d\,(FAR)\frac{3}{2(PW)} \tag{8}$$

where, $\dot{m}_{delivery}$ is the injector delivery rate (g sec^{-1}), ℓ_{ref} the reference density used to calculate volumetric efficiency (kg m^{-3}), FAR is the fuel air ratio and Pw is the injection duration (°CA).

The four cylinders were then connected together through the engine part which translates the force acting on each piston into the crankshaft (brake) power. In the engine model: engine type was 4-stroke type; the number of cylinders is set to four; the configuration inline had been chosen; and simulation with prescribed engine speed was specified rather than engine load. Furthermore, engine friction model was imposed to model friction in the engine. The Friction Mean Effective Pressure (FMEP) was modeled based on Eq. 9:

$$FMEP = 0.4+(0.005\times P_{max})+(0.09\times speed_{mp})+(0.0009\times speed^2_{mp}) \tag{9}$$

where, $Speed_{mp}$ represents the mean piston speed and P_{max} is the peak cylinder pressure.

Engine model: The engine model for an in-line 4-cylinder direct injection engine was developed for this study. Engine specifications for the base engine are tabulated in Table 1. The specific values of input parameters including the AFR, engine speed and injection timing were defined in the model. The boundary condition of the intake air was defined first in the entrance of the engine. The air enters through a bell-mouth orifice to the pipe. The discharge coefficients of the bell-mouth orifice were set to 1 to ensure the smooth transition as in the real engine. The pipe of bell-mouth orifice with 0.07 m of diameter and 0.1 m of length are used in this model. The pipe connects in the intake to the air cleaner with 0.16 m of diameter and 0.25 m of length was modeled. The air cleaner pipe identical to the bell-mouth orifice connects to the manifold. A log style manifold was developed from a series of pipes and flow-splits. The intake system of the present study model is shown in Fig. 1. The total volume for each flow-split was 256 cm^3. The flow-splits compose from an intake and two discharges. The intake draws air from the preceding flow-split. One discharge supplies air to adjacent intake runner and the other supplies air to the next flow-split. The last discharge pipe was closed with a cup to prevent any flow through it because there is no more flow-split. The flow-splits are connected with each other via pipes with 0.09 m diameter and 0.92 m length. The junctions between the flow-splits and the intake runners were modeled with bell-mouth orifices. The discharge coefficients were also set to 1 to assure smooth transition, because in most manifolds the transition from the manifold to the runners is very smooth. The intake runners for the four cylinders were modeled as four identical pipes with. 04 m diameter and 0.1 m length. Finally the intake runners were linked to the intake ports which were modeled as pipes with 0.04 m diameter and 0.08 length. The air mass flow rate in e intake port was used for hydrogen flow rate based on the imposed AFR.

The second major part of the engine model is the powertrain model which is shown in Fig. 2. In the powertrain, the induced air passes through the intake

Table 1: Engine specification

Engine parameter	Value	Unit
Bore	100	mm
Stroke	100	mm
Connecting rod length	220	mm
Piston pin offset	1.00	mm
Total displacement	3142	(cm^3)
Compression ratio	9.5	
Inlet valve close, IVC	-96	^{0}CA
Exhaust valve open, EVO	125	^{0}CA
Inlet valve open, IVO	351	^{0}CA
Exhaust valve close, EVC	398	^{0}CA

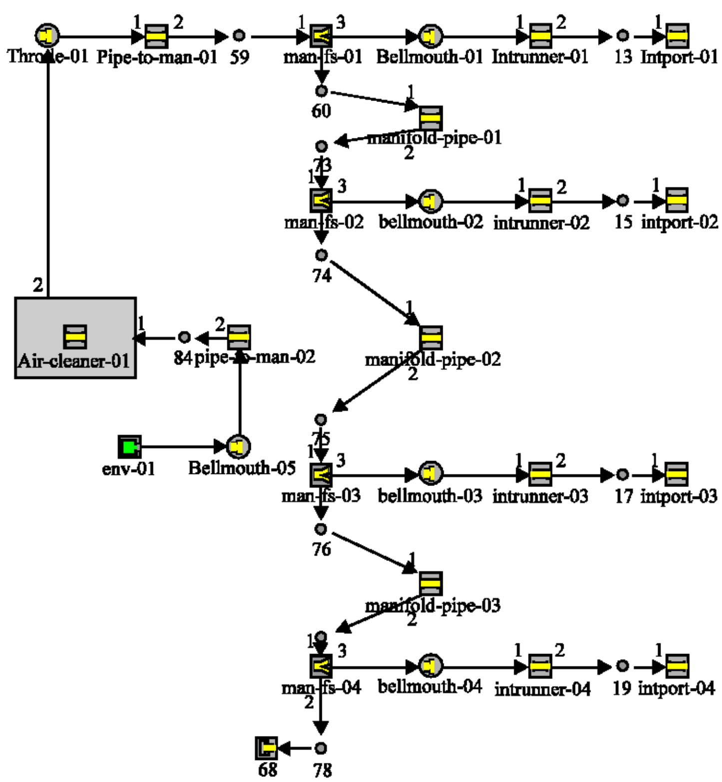

Fig. 1: Intake system model

cam-driven type valves with 45.5 mm of diameter to the cylinders. The valve lash (mechanical clearance between the cam lobe and the valve stem) was set to 0.1 mm. The overall temperature of the head, piston and cylinder for the engine parts are listed in Table 2. The temperature of the piston is higher than the cylinder head and cylinder block wall temperature because this part is not directly cooled by the cooling liquid or oil.

The last major part in the present model is the exhaust system which is shown in Fig. 3. The exhaust runners were modeled as rounded pipes with 0.03 m inlet diameter and 80^0 bending angle for runners 1 and 4; and 40° bending angle of runners 2 and 3. Runners 1 and 4 and runners 2 and 3 are connected before enter in a flow-split with 169.646 cm^3 volume. Conservation of momentum is solved in 3-dimentional flow-splits even though the flow in GT-Power is otherwise based on a one-dimensional version of the Navier-Stokes equation. Finally, a pipe with 0.06 m diameter and 0.15 m length connects the last flow-split to the environment. Exhaust system walls temperature was calculated using a model embodied in each pipe and flow-split. Table 3 are listed the parameters used in the exhaust environment of the model.

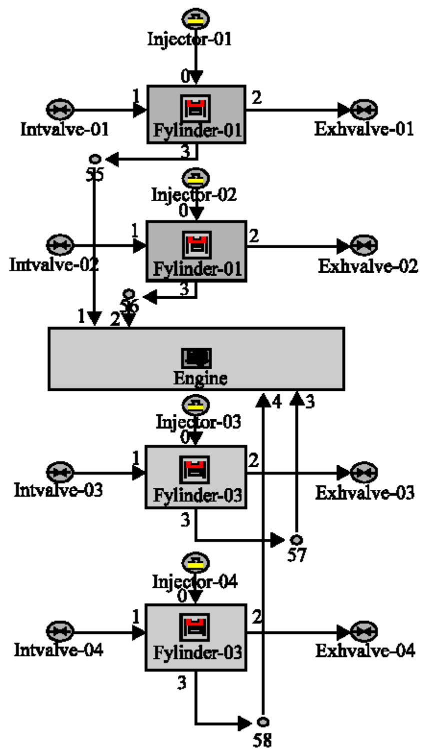

Fig. 2: Powertrain model

Table 2: Temperature of the mail engine parts

Components	Temperature (K)
Cylinder head	550
Cylinder block wall	450
Piston	590

Table 3: Parameters used in the exhaust environment

Parameters	Value	Unit
External environment temperature	320	K
Heat transfer coefficient	15	W/m^2K
Radiative temperature	320	K
Wall layer material	Steel	
Layer thickness	3	mm
Emissivity	0.8	

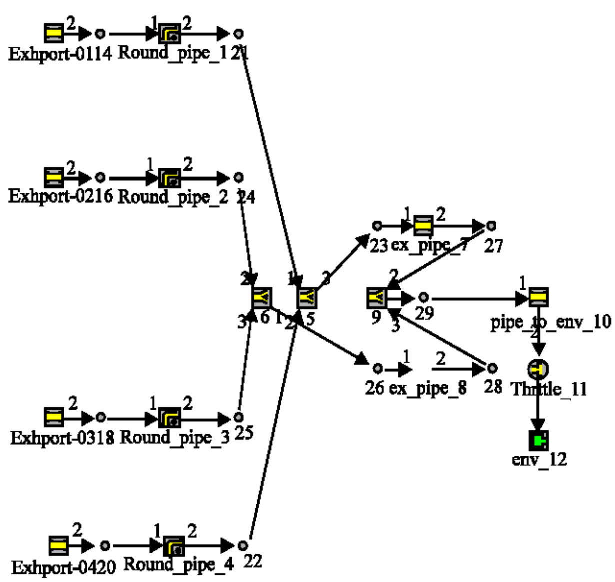

Fig. 3: Exhaust system model

RESULTS

It is worthy to mention that one of the most attractive combustive features for hydrogen fuel is its wide range of flammability. A lean mixture is one in which the amount of fuel is less than stoichiometric mixture. This leads to fairly easy to get an engine start. Furthermore, the combustion reaction will be more complete. Additionally, the final combustion temperature is lower reducing the amount of pollutants. The air-fuel ratio AFR was varied from rich limit (AFR = 27.464:1 based on mass where the equivalence ratio (ϕ = 1.2) to a very lean limit (AFR =171.65 where (ϕ = 0.2) and engine speed varied from 2500 to 4500 rpm. BMEP is a good parameter for comparing engines with regard to design due to its independent on the engine size and speed.

Variation in air fuel ratio on engine performance: Figure 4 shows the effect of air-fuel ratio on the brake mean effective pressure. It can be seen that BMEP decreases with increases of AFR and speed. This decrease happens with two different behaviors. For rich mixtures (low AFR), BMEF decreases almost linearly, then BMEP falls with a non-linear behavior. Higher linear range can be recognized for higher speeds. For 4500 rpm, the linear range is continuing until AFR of 42.9125 (ϕ =0.8). The non-linear region becomes more predominant at lower speeds and the linear region cannot be specified there. The total drop of BMEP within the studied range of AFR was 8.08 bar for 4500 rpm compared with 10.91 bar for 2500 rpm. At lean operating conditions (AFR = 171.65, (ϕ = 0.2 the engine gives maximum power (BMEP = 1.635 bar) at lower speed 2500 rpm) compared with the power (BMEP = 0.24 bar) at speed 4500 rpm.

Figure 5 shows the variation of the brake thermal efficiency with the air fuel ratio for the selected speeds. Brake power is the useful part as a percentage from the intake fuel energy. The fuel energy is also covered the friction losses and heat losses (heat loss to surroundings, exhaust, enthalpy and coolant load). Therefore, lower values of ηb can be seen in Fig. 5. It can be observed that the brake thermal efficiency is increases nearby the richest condition (AFR ≅ 35) and then decreases with increases of AFR and speed. The operation within a range of AFR from 38.144 to 42.91250 (ϕ = 0.9-0.8) gives the maximum values for ηb for all speeds. Maximum ηb of 35.4% at speed 2500 rpm can be seen compared with 26.3% at speed 4500 rpm. Unaccepted efficiency ηb of 3.7% can be seen at very lean conditions with AFR of 171.65 (ϕ = 0.2 for speed of 4500 rpm, while a value of 23.86% was recorded at the same conditions with speed of 2500 rpm. Clearly, rotational speed has a major effect in the behavior of η_b with AFR. Higher speeds lead to higher friction losses.

Figure 6 depicts the behavior of the brake specific fuel consumption BSFC with AFR. It is easy to perceive from the Fig. 6 that there is an optimum minimum value of BSFC occurred within a range of AFR from 38.144 (ϕ = 0.9) to 49.0428 (ϕ = 0.7) for the selected range of speed. At very lean conditions, higher fuel consumption can be noticed. After AFR of 114.433 (ϕ = 0.3) the BSFC rises up rapidly, especially for high speeds. At very lean conditions with AFR of 171.65 (ϕ = 0.2), a BSFC of 125.87 g kW h^{-1} was observed for the speed of 2500 rpm; while it was 809 g kW h^{-1} for 4500 rpm.

Figure 7 shows how the AFR can affect the maximum temperature inside the cylinder. In general, lower temperatures are required due to the reduction of pollutants. It is clearly demonstrated how the increase in the AFR can decrease the maximum cylinder temperature with a severe steeped curve. But for rich mixtures, the

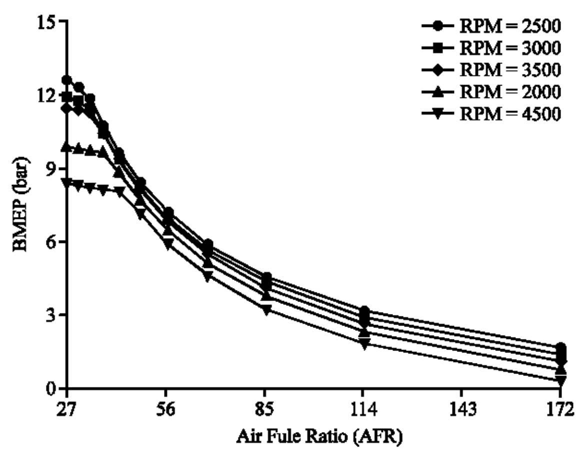

Fig. 4: Variation of brake mean effective pressure with air fuel ratio for various engine speeds

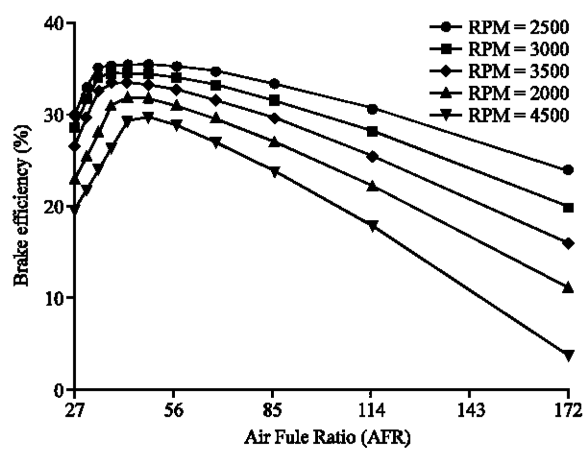

Fig. 5: Variation of brake thermal efficiency with air fuel ratio

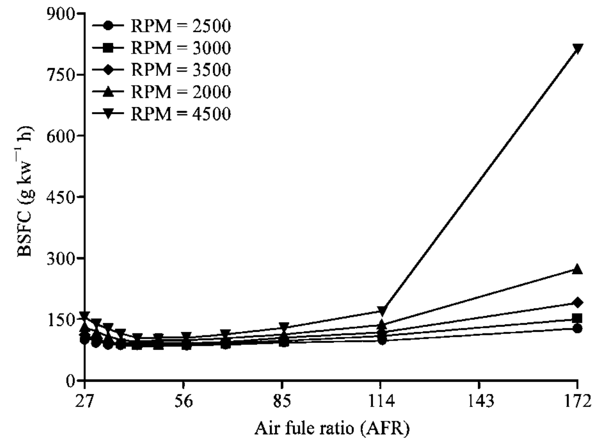

Fig. 6: Variation of brake specific fuel consumption with air fuel ratio for different engine speed

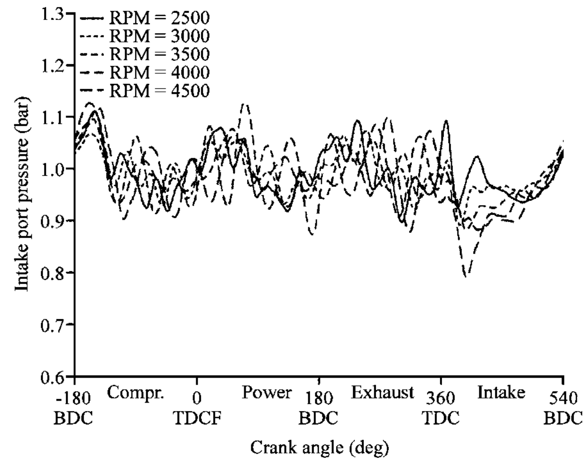

Fig. 8: Instantaneous intake port pressure distributions with crank angle for different speed

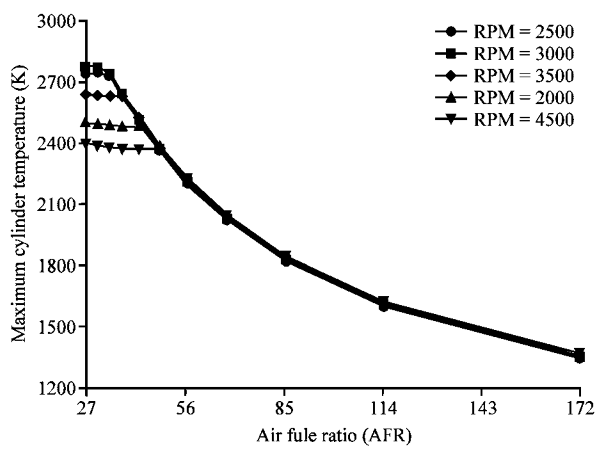

Fig. 7: Variation of maximum cylinder temperature with air fuel ratio

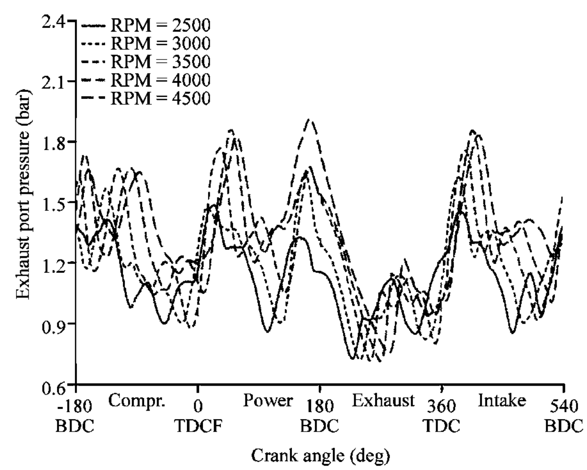

Fig. 9: Instantaneous exhaust port pressure distributions with crank angle for various engine speeds

maximum cylinder temperature drops down with a linear manner. The effect of the engine speed on the relationship between maximum cylinder temperatures with AFR seems to be minor. At rich operating conditions (AFR = 27.464, ϕ = 1.2) and a speed of 3000 rpm, a maximum cylinder temperature of 2767 K was recorded. This temperature dropped down to 1345 K at AFR of 171.65 (ϕ = 0.2). This lower temperature inhibits the formation of NO_x pollutants. In fact this feature is one of the major motivations toward hydrogen fuel.

Instantaneous behaviour on crank angle: The intake port and exhaust port pressures in terms of crank angle are shown in Fig. 8 and 9, respectively. The gas dynamic effects play a very important rule here. It distorts the exhaust flow which is shown in Fig. 9. The rise of the pressure at the end of the exhaust stroke can lead to reverse flow into the cylinder past the exhaust valve; however, the high vacuum in the beginning of the first stroke is highly desired to banish the burnt gases out of the cylinder. At speed of 3000 rpm, a maximum pressure of 1.64 bar and maximum vacuum of 0.72 bar were recorded. The response of fluctuation of the amplitude to the engine speed in case of exhaust pressure seems to be less than the intake pressure. But the fluctuation is also increasing with the increase of the engine speed.

Figure 10 shows the behavior of the cylinder pressure at the last cycle (12th cycle) for WOT and stoichiometric operation conditions. The behavior of the pressure follows the combustion phenomenon that occurs. The effect of the rotational speed on the instantaneous behavior of the cylinder pressure is minor.

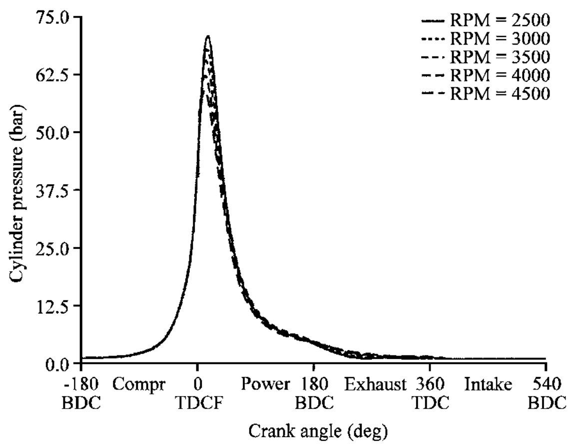

Fig. 10: Instantaneous cylinder pressure distributions with crank angle for various engine speed

The maximum pressure has been observed at engine speed of 2500 rpm however the minimum pressure was obtained at 4500 rpm.

DISCUSSION

It has been adequately emphasized that hydrogen fuel possesses some properties which are uniquely different from the corresponding properties of conventional hydrocarbon fuels. This was primarily the reason why initially the research and development work on. The symptoms of unsteady combustion the most pronounced effect in an internal combustion engine. Hydrogen has long since been attempted as a fuel for the internal combustion engine. In general, it is desirable to have maximum volumetric efficiency for engine. The importance of efficiency is more critical for hydrogen engines because of the hydrogen fuel displaces large amount of incoming air due to its low density (0.0824 kg m^{-3} at 25°C and 1 atm.). This reason reduces the efficiency to high extent. A stoichiometric mixture of hydrogen and air consists of approximately 30% hydrogen by volume, whereas a stoichiometric mixture of fully vaporized gasoline and air consists of approximately 2% gasoline by volume (White *et al*., 2006). Therefore, the low efficiency for hydrogen engine is expected compared to gasoline engine works with same operating conditions and physical dimension. However, the higher efficiencies can be gained with direct injection of hydrogen, which can be shown in Fig. 5. The maximum value of efficiency for the selected range of speed was around 85%. At further higher engine speed beyond these values, the flow into the engine during at least part of the intake process becomes chocked. Once this condition occurs, further increases in engine speed decrease the flow rate significantly. Thus, the efficiency decreases sharply because of the higher speed is accompanied by some phenomenon that have negative influence on efficiency. These phenomenon include the charge heating in the manifold and higher friction flow losses which increase as the square of engine speed. Due to dissociation at high temperatures following combustion, molecular oxygen is present in the burned gases under stoichiometric conditions. Thus, some additional fuel can be added and partially burned. This increases the temperature and the number of moles of the burned gases in the cylinder. These effects increases the pressure were given increase power and mean effective pressure (Ferguson and Kirkpatrick, 2001).

The AFR for optimum fuel consumption at a given load depends on the details of chamber design (including compression ratio) and mixture preparation quality. It varies for a given chamber with the part of throttle load and speed range (Ferguson and Kirkpatrick, 2001). It is clearly seen (Fig. 6) that the higher fuel is consumed at higher speeds due to the greater friction losses that can occur at high speeds. The value BSFC at speed of 2500 rpm was doubled around two times at speed of 4000 rpm; however the same value was doubled around five times at speed of 4500 rpm. This is because of very lean operation conditions can lead to unstable combustion and more lost power due to a reduction in the volumetric heating value of the air/hydrogen mixture.

The instantaneous behavior is at the 12th cycle for Wide Open Throttle (WOT) and stoichiometric operation. These Fig. 8 and 9 are very important to investigate the backfire or pre-ignition occurrence in details. However, for the present case there is neither backfire nor pre-ignition and this is the case of normal combustion and shows typical results of pressure variation. The crank angle axis is divided into four parts to indicate the four strokes which take two cycles (720 degrees). The pressure seems to be a series of pulses. Each pulse is approximately sinusoidal in shape. The complexity of the phenomena that occur is apparent. Back flow from the cylinder into the intake manifold can be recognized during the early part of the intake process until the cylinder pressure falls below the manifold pressure. This happens within about 40 crank angle degrees and stops when the angle crank reaches 400 degree from the life cycle. Backflow also occur early in the compression stroke before the inlet valve closed due to rising cylinder pressure. The amplitude of the pressure fluctuations increases substantially with increasing engine speed. From Fig. 8, the maximum intake pressure was recorded 1.1 bar at speed 4500 rpm during the compression stroke, while it was 1.093 bar at speed of 2500 rpm. At the intake stroke, when high intake vacuum is occurred, the flow is continuously inward and flow pulsation is small. For high speed, larger pulses can be seen. At high speeds more fuel is required and consequently more vacuum in the intake port. A vacuum of 0.792 bar was calculated in 4500 rpm compared with 0.925 bar at 2500 rpm.

The behavior of the pressure follows the combustion phenomenon that occurs. The effect of the rotational speed on the instantaneous behavior of the cylinder pressure is minor. This curve can be divided into three parts for discussion purpose. The first part corresponds the flame development period which consumes about 5% of the air fuel mixture. Very little pressure rise is noticeable and little or no useful work is produced. The second part corresponds the flame propagation period which consumes about 90% of the mixture. During this time, pressure in the cylinder is greatly increased, providing the force to produce work in the expansion stroke. The third part corresponds to flame termination period which consumes about the rest of the mixture (5%). In general this behavior is like the behavior of the traditional gasoline fuel, however it is necessary to keep in mind that during the hydrogen combustion, the flame velocity is rapid and the main changes of cylinder pressure (the second part) occur in a shorter time. Whilst experimental data are not available to verify these predictions, the authors are presented here to illustrate some of the insights that this type of simulation tool may provide to future engine systems designers.

CONCLUSIONS

The present study considered the performance characteristics of a four cylinders hydrogen fueled internal combustion engine with hydrogen being injected directly in the cylinder. The following conclusions are drawn:

- At very lean conditions with low engine speeds, acceptable BMEP can be reached, while it is unacceptable for higher speeds. Lean operation leads to small values of BMEP compared with rich conditions
- Maximum brake thermal efficiency can be reached at mixture composition in the range of (ϕ = 0.9 to 0.8) and it decreases dramatically at leaner conditions
- The desired minimum BSFC occurs within a mixture composition range of (ϕ = 0.7 to 0.9). The operation with very lean condition (ϕ<0.2) and high engine speeds (>4500) consumes unacceptable amounts of fuel
- Lean operation conditions results in lower maximum cylinder temperature. A reduction of around 1400 K can be gained if the engine works properly at (ϕ<0.2) instead of stoichiometric operation
- Hydrogen combustion results in moderate pressures in the cylinder. This reduces the compactness required in the construction of the engine. But, if abnormal combustion like pre-ignition or backfire happens, higher pressures may destroy the connecting rod and piston rings. Therefore, much care should be paid for this point

ACKNOWLEDGMENT

The authors would like to express their deep gratitude to Universiti Malaysia Pahang (UMP) for provided the laboratory facilities and financial support under project No. RDU 08-05-074.

REFERENCES

Blair, G.P., 1999. Design and Simulation of Four Stroke Engines. SAE International. Society of Automotive Engineers Inc. Warrandale, Pa., USA., ISBN: 978-0-7680-0440-3, pp: 1-840.

COD (College of the Desert), 2001. Hydrogen fuel cell engines and related technologies, module 3: Hydrogen use in internal combustion engines. http://www1.eere.energy.gov/hydrogenandfuelcells/tech_validation/h2_manual.html.

Ferguson, C.R. and A.T. Kirkpatrick, 2001. International Combustion Engines: Applied Thermosciences. 2nd Edn., John Wiley and Sons, Inc., New York, pp: 1-384.

Green, R.K. and N.D. Glasson, 1992. High-pressure hydrogen injection for internal combustion engines. Int. J. Hydrogen Energy, 17: 895-901.

Guo, L.S., H.B. Lu and J.D. Li, 1999. A hydrogen injection system with solenoid valves for a four cylinder hydrogen-fuelled engine. Int. J. Hydrogen Energy, 24: 377-382.

Heywood, J.B., 1988. Internal Combustion Engine Fundamentals. 1st Edn. McGraw-Hill, New York, ISBN: 0-07-028637-X.

Homan, H.S., P.C.T. De Boer and W.J. McLean, 1983. The effect of fuel injection on NOx emissions and undesirable combustion for hydrogen-fuelled piston engines. Int. J. Hydrogen Energy, 8: 131-146.

Jorach, R., E. Christian and D. Ralf, 1997. Development of a low-NOx truck hydrogen engine with high specific power output. Int. J. Hydrogen Energy, 22: 423-427.

Kim, J.M., Y.T. Kim, J.T. Lee and S.Y. Lee, 1995. Performance characteristics of hydrogen fueled engine with the direct injection and spark ignition system. SAE Paper No. 952498. http://www.sae.org/technical/papers/952498.

Kim, Y.Y., J.T. Lee and J.A. Caton, 2006. The development of a dual-Injection hydrogen-fueled engine with high power and high efficiency, J. Eng. Gas Turbines Power, ASME, 128: 203-212.

Mohammadi, A., M. Shioji, Y. Nakai, W. Ishikura and E. Tabo, 2007. Performance and combustion characteristics of a direct injection SI hydrogen engine. Int. J. Hydrogen Energy, 32: 296-304.

Rottengruber, H., M. Berckmüller, G. Elsässer, N. Brehm and C. Schwarz, 2004. Direct-injection hydrogen SI-engine operation strategy and power density potentials. http://www.sae.org/technical/papers/2004-01-2927.

Stockhausen, W.F., R.J. Natkin, D.M. Kabat, L. Reams, X. Tang and S. Hashemi, 2002. Ford P2000 hydrogen engine design and vehicle development program. SAE paper 2002; 2002-01-0240. http://www.sae.org/technical/papers/2002-01-0240.

Suwanchotchoung, N., 2003. Performance of a spark ignition dual-fueled engine using split-injection timing. Ph.D. Thesis, Vanderbilt University, Mechanical Engineering.

Tsujimura, T., A. Mikami and N. Achiha, 2003. A study of direct injection diesel engine fueled with hydrogen. SAE paper no. 2003-01-0761.

Verhelst, S., 2005. A study of the combustion in hydrogen-fuelled internal combustion engines. Ph.D Thesis, Department of Mechanical Engineering, Ghent University.

Verhelst, S., R. Sierens and S. Verstraeten, 2006. A critical review of experimental research on hydrogen fueled SI engines. http://www.sae.org/technical/papers/2006-01-0430.

White, C.M., R.R. Steeper and A.E. Lutz, 2006. The hydrogen-fueled internal combustion engine: A technical review. Int. J. Hydrogen Energy, 31: 1292-1305.

Yi, H.S., S.J. Lee and E.S. Kim, 1996. Performance evaluation and emission characteristics of in-cylinder injection type hydrogen fueled engine. Int. J. Hydrogen Energy, 21: 617-624.

Yi, H.S., K. Min and E.S. Kim, 2000. The optimised mixture formation for hydrogen fuelled. Int. J. Hydrogen Energy, 25: 685-690.

Zhenzhong, Y., W. Jianqin, F. Zhuoyi and L. Jinding, 2002. An investigation of optimum control of ignition timing and injection system in an in-cylinder injection type hydrogen fueled engine. Int. J. Hydrogen Energy, 27: 213-217.